ELSEVIER

Catalysis Today 77 (2003) 315–323

CATALYSIS TODAY

www.elsevier.com/locate/cattod

Preparation and characterisation of mesoporous silica–alumina and silica–titania with a narrow pore size distribution

A. Carati [a], G. Ferraris [b], M. Guidotti [c,*], G. Moretti [b], R. Psaro [c], C. Rizzo [a]

[a] *EniTecnologie, Via Maritano 26, 20097 San Donato Milanese, MI, Italy*
[b] *CNR-IMIP and Dipartimento di Chimica, Università "La Sapienza", p.le A. Moro 5, 00185 Roma, Italy*
[c] *CNR-ISTM, via C. Golgi 19, 20133 Milano, Italy*

Abstract

Amorphous mesoporous materials with a different degree of order in the arrangement of pores are outlined. Particularly, the synthesis of a class of mesoporous silica–alumina (MSA) materials with narrow pore size distribution and a disordered arrangement of pores is reported and discussed. Likewise, the preparation of titanium-containing ordered mesoporous silicates (Ti-MCM-41) and disordered mesoporous silica–titania (MST) are also described in detail. The structural properties of the solids are compared by means of X-ray diffraction and UV-Vis diffuse reflectance spectroscopy. The nitrogen adsorption–desorption measurements were performed and the textural properties are evaluated by the BET, DFT, BJH and *t*-plot methods.

The high specific surface area and pore volume, as well as the acidity, make MSA solids interesting catalysts in several petrochemical transformations, i.e. oligomerisation, alkylation, hydroisomerisation, rearrangement reactions. Besides, thanks to the width of the mesopores of such solids, the catalytic activity of titanium-containing silicates may have a potential application in the epoxidation of bulky unsaturated fine chemical substrates.

Keywords: Silica–alumina; Silica–titania; Pore size distribution; Mesoporous materials

1. Introduction

The ever-growing importance of inorganic materials with controlled pore size distribution is mainly due not only to the deep theoretical interest on such compounds, but also to the wide number of applications in which they are employed (not only in catalysis) [1].

The most important family of this sort of materials are *zeolites*. Their three-dimensional crystalline framework is formed by corner-sharing SiO_4 tetrahedra, with the possibility to replace a few SiO_4 units by AlO_4^- units, and protons or an equivalent amount of cations to maintain the electronic neutrality of the structure. They are characterised by a very narrow pore size distribution in the micropore region and, because of this unique feature, they are also called molecular sieves, as they act a *shape selectivity* on the substrate molecules which go in, go out or are formed in the porous network. Actually, molecules with a size smaller than or similar to the diameter of the pores are allowed into the internal cavities, whereas bulkier molecules are not.

Nevertheless, even on the large-pore microporous zeolites, such as FAU (zeolites X and Y), or BEA (zeolite beta), there are severe limitations for the size of molecules that can be subjected to shape-selective reactions. The situation changed when researchers

* Corresponding author.
E-mail address: mguidotti@csmtbo.mi.cnr.it (M. Guidotti).

0920-5861/02/$ – see front matter © 2002 Elsevier Science B.V. All rights reserved.
PII: S0920-5861(02)00376-0

at the Mobil Laboratories announced in 1992 the discovery of a family of mesoporous solids with pore diameters ranging from some 2 to 10 nm [2,3] and large and accessible internal areas (higher than $600\,m^2\,g^{-1}$). Instead of using single molecules as templates, like in the case of the microporous zeolite synthesis, the chemists from Mobil employed supramolecular long-range ordered aggregates of surfactant micelle molecules. The use of these lyotropic phases leads to mesostructured materials (silicates, aluminosilicates) with different structure types. After calcination, these precursors leave mesoporous materials with an *ordered arrangement of pores*. Such materials, designed as M41S, are not crystalline and their pore size distribution is broader and tunable in a larger range of porosity with respect to microporous zeolites. Other amorphous silica–alumina materials, prepared by surfactant micelle templated syntheses and characterised by a narrow pore size distribution in mesopore region, have been described by several research groups: FSM-16 [4], HMS [5], SBA [6], MSU [7], KIT-1 [8]. Acting as proper molecular sieves in the mesoporous range, these solids are currently being tested in several applications, which are analogous to those of microporous zeolites and zeotypes [9].

New mesoporous silica–alumina (MSA) materials with narrow pore size distributions, but with a *disordered arrangement*, have also been described. These materials do not therefore show the X-ray diffraction pattern in the low 2θ region characteristic of the M41S materials. Such structures were first developed by researchers of EniTecnologie [10,11] and designated with the acronym MSA. MSA is the amorphous precursors of ZSM-5 zeolite synthesised in the presence of tetrapropylammonium hydroxide (TPA-OH) from alkali-free solutions. The presence of TPA clusters in the MSA precursors are responsible for the formation of mesopores, whilst isolated TPA^+ ions, acting as counterions to the tetrahedrally coordinated Al ions, would account for the formation of micropores, as occurs in ZSM-5 crystals.

The interest of inorganic materials with a well-defined pore size distribution rests on several reasons [1,12–14]:

(i) The void space on the total volume of the solid is 30–50% for zeolites, and 50–80% for mesoporous materials.
(ii) The large and accessible internal surface can contain several types of active sites: Lewis and Brønsted acids, transition metal ions, nanometric metal clusters. When the concentration of the active species is relatively small, the active sites bound to the surface do not interact among them, so that they are highly dispersed, virtually single active sites.
(iii) In situ studies of chemical reactivity within the channels and cavities of the catalysts can be quantitatively followed by a range of powerful physico-chemical techniques.
(iv) Computational methods based on quantum chemical techniques and classical methods of lattice-energy minimisation and computer graphics may contribute to rationalise the structural and chemical properties of such catalysts.
(v) Many elements of the periodic table can be incorporated into the network or easily exchanged at the extra-framework positions.

With regard to the latter topic, many heterogeneous catalysts have been reported in the past to be prepared by anchoring or grafting processes. The general meaning of these terms is that covalent bonds are formed between a homogeneous transition metal complex and an inert polymer or inorganic support [15]. The aim is to combine the potential versatility and selectivity of homogeneous catalysts with the practical advantages of a solid material. According to Campbell, an anchored catalysts is created by the binding of a species, without substantial change in its structure, to a solid surface [16]. A grafted catalyst is produced when an initial structure bound to the surface is altered considerably by subsequent treatments. Whenever the initially bound species is not an active catalytic species, the definition implies that anchoring necessarily occurs before grafting can take place.

In last decades, thanks to the growing attention paid to environmental concerns, microporous materials have gained and still play a very significant role in industrial applications, as catalysts (e.g. ultrastable zeolite Y, ZSM-5, Beta), as sorbents (e.g. zeolites A and X) and as cation exchangers (e.g. zeolite A) [1,12,13]. The use of such solids as heterogeneous catalysts allows a reduction in the use of stoichiometric amounts of reagents, limits the waste by-product formation and simplifies the catalyst separation and

recycling processes. More recently, mesoporous materials with controlled pore size distribution were developed and, even if industrial applications have not been realised up to now, they are extensively studied. These materials, thanks to the large dimensions of their channels, are particularly suitable for application in those fine chemical transformation processes, in which the environmental impact is still relevant [17].

In particular, for MSA type mesoporous silica–alumina some catalytic applications have been developed till pilot plant (olefin oligomerisation and catalytic dewaxing). Likewise, mesoporous titanium-containing silicates, thanks to the good performances displayed in the selective oxidation of fine chemistry substrates, may be considered as a valid alternative to the use of hazardous amounts of inorganic oxidants or organic peroxoacids.

In this paper, the syntheses and properties of mesoporous aluminium-silicates of MSA type and titanium-silicates of MCM-41 and mesoporous silica–titania (MST) type will be described. These materials are characterised by a different degree of order in the arrangement of pores. The structural properties of the solids are compared by means of X-ray Diffraction and UV-Vis analysis. The nitrogen adsorption–desorption measurements were performed and the textural properties were evaluated by the BET, DFT, BJH and *t*-plot methods.

2. Experimental section

2.1. Catalyst preparation

2.1.1. MSA and MST

MSA and MST were prepared as previously described [11,18]. As precursors of MFI structure zeolites, they were obtained in presence of tetrapropylammonium hydroxide (TPA-OH) from an alkali-free reagent mixture.

The samples were prepared from tetraethyl orthosilicate $Si(OC_2H_5)_4$ (Dynasil A, Nobel), tetrapropylammonium hydroxide (TPA-OH; Sachem), water and eventually ethanol and triisopropyl orthoaluminate $Al(iso\text{-}OC_3H_7)_3$ (Fluka) or tetraethyl orthotitanate $Ti(OC_2H_5)_4$ (Fluka).

The siliceous and aluminosilicate MSA samples were prepared from reagent mixtures having the following molar compositions:

MSA-1 SiO_2: TPA-OH : H_2O = 1:0.1:15

MSA-2 SiO_2: Al_2O_3: TPA-OH : H_2O = 1:0.01:0.1:15

MSA-3 SiO_2: Al_2O_3: TPA-OH : H_2O : EtOH = 1:0.01:0.1:8:8

$Al(iso\text{-}OC_3H_7)_3$ was dissolved at 333 K in TPA-OH (12 wt.% in aqueous solution). The solution was cooled to room temperature, then $Si(OC_2H_5)_4$ was added. The sol was charged in a stainless steel autoclave and kept at 358 K under autogenous pressure for 3 h. A monophasic clear sol was obtained and transformed in a opalescent homogeneous gel by solvent evaporation.

The last synthesis was performed with added ethanol and gelled at room temperature obtaining directly an opalescent homogeneous gel. After 15 h ageing at room temperature, the gels were dried at 373 K and calcined for 8 h in air at 823 K.

The MST sample was prepared by the following molar composition reagent mixture:

MST SiO_2: TiO_2: TPA-OH : H_2O = 1:0.031:0.1:20

According to Corma et al. [19,20], alkali metal cations were carefully excluded because they could impede the insertion of Ti(IV) into the silicate framework, as occurs in the case of the TS-1 preparation. A clear sol with a pH around 12 was obtained by adding $Si(OC_2H_5)_4$ to a 20 wt.% aqueous solution of tetrapropylammonium hydroxide (TPA-OH) containing $Ti(OC_2H_5)_4$. The solution was charged in a stainless steel autoclave and kept at 453 K, without stirring, under autogenous pressure for 30 min. The clear sol was then transformed in a clear dense gel by partial evaporation of the solvent. The powder was recovered and washed by centrifugation. The sample was dried at 363 K for 24 h in air and finally calcined at 823 K in air for 6 h.

2.1.2. MCM-41 and in-framework [Ti]-MCM-41

MCM-41 and [Ti]-MCM-41 (Ti ions in the framework) were synthesised according to the procedures developed by Mobil researchers [2,3] and Corma et al. [19,20], respectively. Some simplifications to

the methodologies were employed after the suggestions reported by Di Renzo et al. [21]. MCM-41 and [Ti]-MCM-41 were prepared using hexadecyltrimethylammonium chloride (CTMA-Cl; Fluka), tetraethyl orthosilicate $Si(OC_2H_5)_4$ (Fluka purum), tetraethyl orthotitanate $Ti(OC_2H_5)_4$ (Aldrich) and ammonia solution (33 wt.%; Allied Signal) [22]. Also in this case alkali metal cations were carefully excluded [19,20].

The molar ratios of the reagent mixtures were the following:

MCM-41 SiO_2: CTMA-Cl : NH_3: H_2O = 1:0.53:18.9:36.2

[Ti]-MCM-41 SiO_2: TiO_2: CTMA-Cl : NH_3: H_2O = 1:0.031:0.53:18.9:36.2

2.1.3. Extra-framework Ti-MCM-41

Ti-MCM-41 (Ti grafted onto the MCM-41 surface) was prepared starting from MCM-41 according to the anchoring/grafting technique proposed by Thomas and co-workers [23,24], using a solution of titanocene dichloride ($Ti(Cp)_2Cl_2$) in chloroform and triethylamine (NEt_3).

The titanium loadings in the samples, determined by ICP-atomic emission spectroscopy, resulted 2.15 wt.% for [Ti]-MCM-41 (Si/Ti = 36), 1.88 wt.% for Ti-MCM-41 (Si/Ti = 41), and 1.79 wt.% for MST (Si/Ti = 42). The Ti loadings are similar to that in ordinary TS-1 catalysts.

2.2. Physico-chemical characterisation

2.2.1. X-ray diffraction analysis

The powder X-ray diffraction analysis was carried out on a Philips automated PW 1729 Diffractometer. The XRD patterns were recorded on the calcined samples (823 K in air for 6 h), as described elsewhere [18,22].

2.2.2. Textural characterisation

The nitrogen isotherms were obtained at liquid nitrogen temperature by using a Micromeritics ASAP 2010 apparatus (static volumetric technique). Before determination of adsorption–desorption isotherms the samples (ca. 0.2 g) were outgassed for 16 h at 623 K under vacuum.

The specific surface area (SSA) has been evaluated by 2-parameters linear BET plot in the range p/p^0 0.01–0.2. The total pore volume ($V_{p\,tot}$) has been evaluated by Gurvitsch rule. BJH method, based on the Kelvin equation, was applied to evaluate mesopore size distribution by desorption branch. For micro-mesoporous materials pore size distributions have been also calculated using DFT method. Indeed, DFT, based on molecular statistical approach, is applied over the complete range of the isotherm and is not restricted to a confined range of relative pressure or pore sizes. Pore size distribution is calculated by fitting the theoretical set of adsorption isotherms, evaluated for different pore sizes, to the experimental results.

2.2.3. UV-Vis characterisation

On titanium-containing materials diffuse reflectance (DRS) UV-Vis spectra were recorded using a Cary 5 spectrometer operating in the wavelength range 200–2500 nm. The spectra were recorded after calcination at 823 K in air and equilibration to the ambient atmosphere.

3. Results and discussion

3.1. X-ray diffraction analysis

All the MSA samples resulted amorphous at powder X-ray diffractometry.

The XRD spectra of MCM-41, [Ti]-MCM-41, Ti-MCM-41 and MST are shown in Fig. 1 (a, b, c and d, respectively). The XRD patterns of MCM-41, [Ti]-MCM-41, Ti-MCM-41 can be indexed in a hexagonal unit cell [18,22]. The interplanar distance (d_{100}) and the hexagonal unit cell parameter ($a = 2d_{100}/\sqrt{3}$) of the samples are reported in Table 1. Ti-MCM-41 is less ordered with respect to MCM-41

Table 1
d_{100} interplanar distances and hexagonal unit cell parameter (a) for the ordered mesoporous Ti-containing zeotypes [18,22]

Sample	d_{100} (nm)	a (nm)
MCM-41	3.56	4.11
[Ti]-MCM-41 (Si/Ti = 36)	3.53	4.08
Ti-MCM-41 (Si/Ti = 41)	3.93	4.54

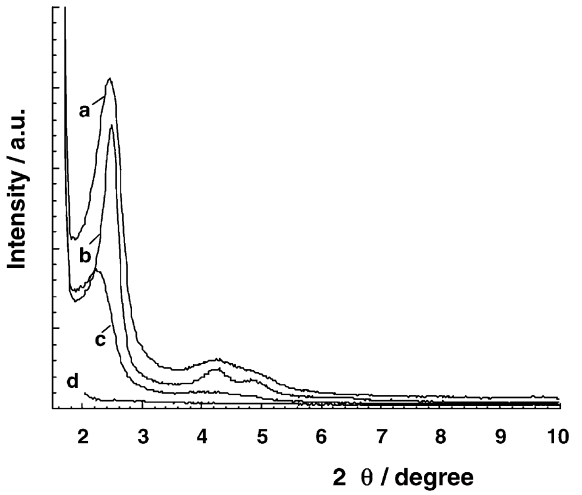

Fig. 1. XRD patterns of MCM-41 (a), [Ti]-MCM-41 (b), Ti-MCM-41 (c) and MST (d) calcined samples.

and [Ti]-MCM-41. MST does not show any peaks in the $1.5 < 2\theta < 10^{\circ}$ range, in agreement with its amorphous nature [25]. Only a broad peak is present at ca. 23°, due to Si(Ti)/Si(Ti) pair correlation [11].

3.2. Textural characterisation

After calcination, MSA-1 and MSA-2 showed irreversible Type I + (IV) isotherms, with a small hysteresis loop. The high adsorption at very low partial pressure <0.1 implies the presence of relevant amount of micropores [8]. The MSA-3 sample showed a IV + (I) isotherm, with a lower adsorption at $p/p^0 < 0.1$ and a higher H2 hysteresis loop with respect to the above samples.

The isotherms and textural properties of the samples are reported, respectively, in Fig. 2 and Table 2.

The presence of alcohol in MSA synthesis is due both to the hydrolysis of alkoxide precursors and

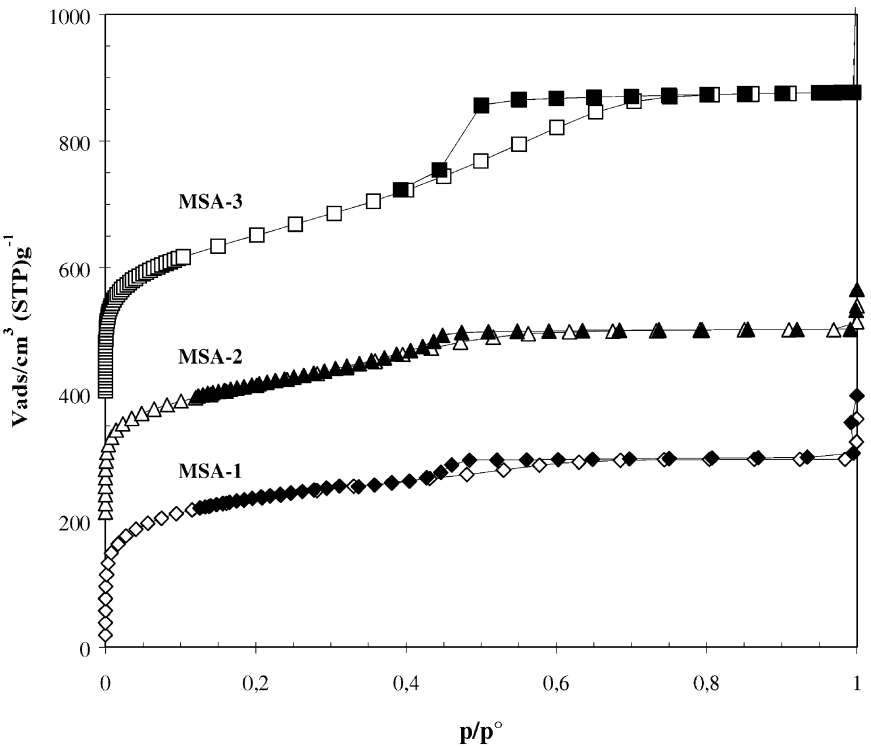

Fig. 2. Nitrogen adsorption–desorption isotherms measured at 77 K of MSA samples. Amount adsorbed for MSA-2 and MSA-3 were incremented by 200, 400 cm^3 (STP) g^{-1}, respectively. Filled symbols denote desorption.

Table 2
Textural properties of the MSA samples

Sample	SSA[a] ($m^2\,g^{-1}$)	$V_{p\,tot}$[b] ($cm^3\,g^{-1}$)	d_{BJH}[c] (nm)	d_{DFT}[c] (nm)
MSA-1(Si)	830	0.46	3.8	2.2
MSA-2(Si-Al-aut)	760	0.47	3.5	2.3
MSA-3(Si-Al-EtOH)	835	0.67	4.0	3.3

[a] BET specific surface area.
[b] Total pore volume.
[c] Mean pore diameter determined by BJH and DFT methods, respectively.

eventually to the addition of free ethanol. In particular, the hydrolysis of $Si(OC_2H_5)_4$ gives rise to a relevant amount of ethanol.

The H_2O/EtOH molar ratio influences the hydrolysis and the successive polymerisation/depolymerisation reactions. As a general rule, hydrolysis is fast and depolymerisation preferred when H_2O/EtOH molar ratio is high [26,27]. For example, a decrease in the pore volume, the surface area and the mean pore size was observed modifying the molar ratio H_2O/EtOH from 1 to 5, for samples gelled at room temperature [27]. Besides, in the present work microporous formation in the samples prepared with the higher H_2O/EtOH ratio is further favoured to the hydrothermal treatment, that gives rise to microporous crystalline zeolite MFI for longer time [8].

Both these effects cause the increase in micropore volume evidenced by both the higher adsorption at low p/p^0 and the lower pore volume with respect to MSA-3 sample.

The presence of added ethanol permits the fast gelation at room temperature of the reagent mixture (in about 5 min). The gelation time can be related to the ability to cross-link polymeric chains. In general, high gelation rates favour the highly branched cluster aggregates of a colloidal nature, giving rise to highly cross-linked mesoporous materials. So the material obtained is mainly mesoporous with a lower contribution of micropores. The H2 hysteresis type is usually attributed either to different size of pore mouth and pore body (this is the case of ink-bottle shaped pores) or to a different behaviour in adsorption and desorption in near cylindrical through pores. The pore dimension values confirm the above speculations: indeed, MSA-1 and MSA-2 show a lower d_{DFT} with respect to MSA-3, due to the large micropore contribution. This causes the observed difference between the pore size determined by BJH and DFT methods.

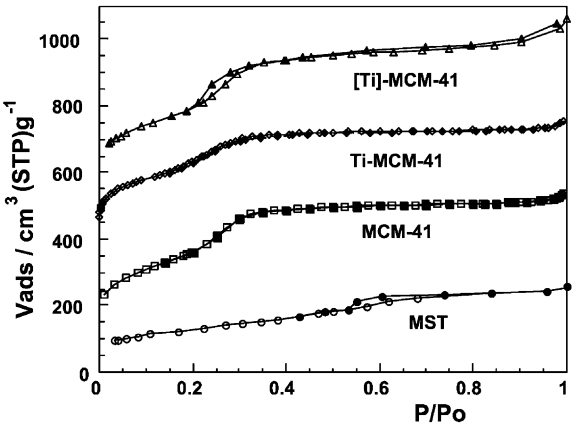

Fig. 3. Nitrogen adsorption–desorption isotherms measured at 77 K of MCM-41, Ti-MCM-41, [Ti]-MCM-41 and MST. Amount adsorbed for MCM-41, Ti-MCM-41 and [Ti]-MCM-41 were incremented by 100, 400 and 550 cm^3 (STP) g^{-1}, respectively. Filled symbols denote desorption.

The N_2 adsorption–desorption isotherms at 77 K of MCM-41, Ti-MCM-41, [Ti]-MCM-41 and MST, are shown in Fig. 3. MCM-41 and Ti-MCM-41, both characterised by ordered cylindrical pores, show completely reversible Type IV isotherms with the inflection in the low relative pressure range (p/p^0 = 0.20–0.35, in this case). This is a peculiar feature of MCM-41 materials, due to the primary mesopore filling step [2,3,28]. The isotherm of [Ti]-MCM-41 showed a hysteresis loop (Fig. 3), indicating that the incorporation of titanium in the MCM-41 framework during its synthesis may lead to the irreversibility of adsorption–desorption behaviour in primary mesopores. A completely different Type IV isotherm is found for MST, characterised by a hysteresis loop displaced at higher p/p^0 values (0.5–0.7).

The results of the isotherms analysis are reported in Table 3. Considering the unit cell parameter (a) reported in Table 1 and the mean pore size (d_{BJH}) reported in Table 3, it is possible to calculate the size of the silicate walls (s) around the hexagonal arrangement of the cylindrical pores by the equation: $a = d_{BJH} + s$. The size of the silicate walls resulted 1.5, 1.8 and 2.1 nm for MCM-41, [Ti]-MCM-41 and Ti-MCM-41, respectively.

Table 3
Textural properties of the ordered and amorphous mesoporous titanium-containing zeotypes

Sample	SSA[a] ($m^2\ g^{-1}$)	$V_{p\,tot}$[b] ($cm^3\ g^{-1}$)	V_μ[c] ($cm^3\ g^{-1}$)	d_{BJH}[d] (nm)
MCM-41	972	0.65	0	2.6
[Ti]-MCM-41	896	0.74	0	2.3
Ti-MCM-41	861	0.53	0	2.4
MST	454	0.38	0	4.6

[a] BET specific surface area.
[b] Total pore volume.
[c] Micropore volume.
[d] Mean pore diameter determined by BJH method.

The increasing size of the pore walls may be correlated to the decrease in the order, as observed for Ti-MCM-41 in the XRD pattern (cf. Fig. 1). The pore size distribution obtained by the BJH method resulted very narrow for all samples, as shown in Fig. 4. The maximum of the distribution corresponds to the diameter reported in Table 3. The reason of the denomination mesoporous molecular sieves for these materials is evident from the results of Fig. 4. A careful *t*-analysis, adopting as a reference a non-porous silica isotherm reported in the literature [29], leads to exclude the presence of micropores in all samples (Table 3), as shown in Fig. 5. The MST catalyst is characterised by a very narrow mesopore size distribution and by the absence of micropores, like the two Ti-containing MCM-41 catalysts and the siliceous MCM-41 support.

3.3. DRS characterisation

The diffuse reflectance UV spectra of [Ti]-MCM-41, Ti-MCM-41 and MST, were reported in Refs. [18,22]. The intense and broad UV absorption bands at ca. 220 nm is due, according to Marchese et al. [30], to oxygen to tetrahedral Ti(IV) ligand to metal charge transfer. This band is affected by the presence of adsorbates [30]. No other spectral features appear and the absence of a band in the range 330–350 nm indicates that any separate TiO_2 (anatase) phase is not present in significant amount in these titanium-containing samples.

3.4. Catalytic applications

Mineral and Lewis acids (i.e. HF, H_2SO_4, $AlCl_3$) are still largely applied as industrial catalysts, e.g. in alkylation, acylation, oligomerisation, rearrangement processes. Their use causes many problems concerning handling, safety, corrosion and waste disposal. The discovery of narrow pore size distribution amorphous silica–alumina materials with acidic or redox-active character, increased the ability to tailor catalysts for selected applications. Such heterogeneous catalysts, as zeolites, can contribute to the greening of chemical

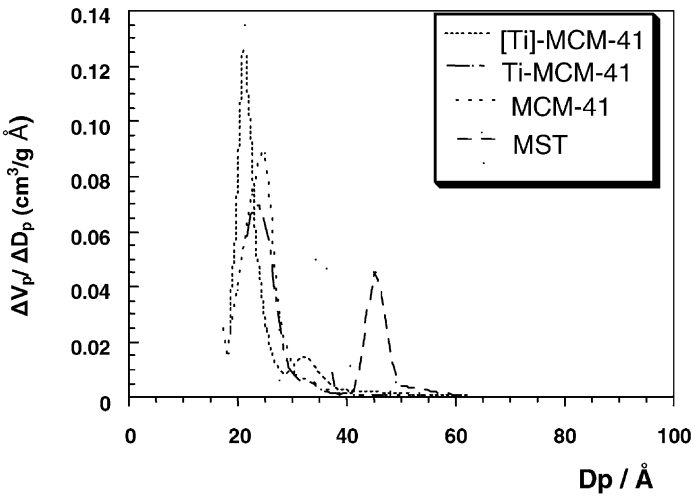

Fig. 4. BJH pore size distribution of ordered MCM-41, Ti-MCM-41, [Ti]-MCM-41 and non-ordered MST samples.

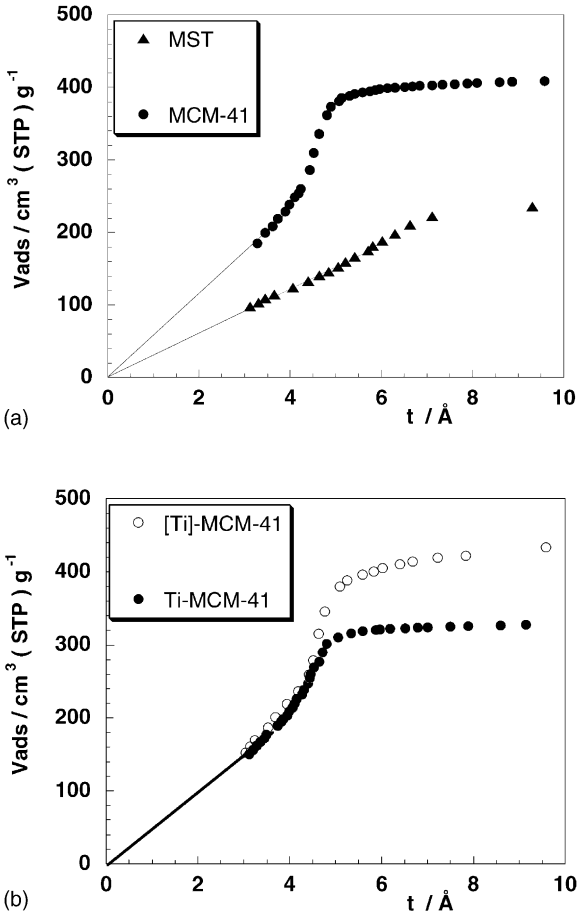

Fig. 5. (a) *t*-Curves of ordered MCM-41 (●) and non-ordered MST (▲) samples; (b) *t*-Curves of ordered [Ti]-MCM-41 (○) and Ti-MCM-41 (●) samples.

industry thanks especially to their shape selectivity behaviour and regenerability.

The use of MSA catalysts in place of traditional acid catalysts was reported in aromatic alkylation [31], oligomerisation of light olefins to gasoline and jet-fuel [32,33] and catalytic rearrangement [34]. The bifunctional catalyst Pt-MSA was described for the wax hydroisomerisation [35]. For example, in the liquid-phase alkylation of toluene with propylene to produce cymenes (a model reaction proposed to identify potential solid acid catalysts for alkylations of industrial interest), MSA showed alkylation activity comparable with zeolite Beta, while isomerisation and transalkylation activities were comparable to that of supported phosphoric acid, but lower than zeolite Beta and $AlCl_3$–HCl [31].

On the other hand, titanium-containing mesoporous molecular sieves are active in oxidation reactions with alkylhydroperoxides. Since in the industrial manufacturing of fine chemicals the selective oxidation transformations are still widely performed by means of large amounts of organic peroxoacids and of transition metal reagents, the use of titanosilicate-based heterogeneous catalysts may contribute remarkably to the setup of environmentally benign industrial processes. The results on the catalytic epoxidation of a series of unsaturated terpenic alcohols on titanium-containing MCM-41 mesoporous materials with *tert*-butylhydroperoxide have been reported [18,22,36]. Under the same experimental conditions, the microporous TS-1 catalyst showed a very good selectivity to epoxidised products, but a very low specific activity. Such a behaviour is consistent with the fact that in TS-1 only a small fraction of titanium sites is effectively active due to the steric limitation imposed by the MFI structure. A direct comparison between in-framework [Ti]-MCM-41 and titanium-grafted Ti-MCM-41 showed a better performance of the latter, thanks to the better exposure of the catalytic sites in the grafted material [22]. MST, likewise, displayed interesting catalytic features in the liquid-phase epoxidation reaction [18]. The titanium-grafted Ti-MCM-41 catalyst was also employed in a bifunctional conversion from citronellal to isopulegol epoxide, in which the acidic character of the titanium site was exploited together with its epoxidation activity [36]. The latter case is therefore an example of multifunctional catalysis, since both the acid-catalysed isomerisation and the epoxidation steps are brought about on the same active site. Such kind of ‘one-pot’ reactions allows a minimisation of the separation of intermediate chemicals and helps in achieving high selectivity and minimal by-product formation [17].

4. Conclusions

The synthesis methodologies of three aluminium-containing (MSA-1, MSA-2 and MSA-3) and three titanium-containing mesoporous materials (MST, [Ti]-MCM-41 and Ti-MCM-41) were reported and discussed. In all cases solids with high specific surface

area, high pore volume and a narrow pore size distributions were obtained. The textural features of such materials can be finely tuned by varying the preparation conditions and their shape-selective properties can be modulated according to the catalytic application in which they may be employed. In presence of titanium precursors redox-active non-ordered mesoporous molecular sieves, named MST, are obtained.

It is also worth underlining that the non-ordered mesoporous aluminosilicate MSA and titanosilicate MST are obtained by means of synthesis methodologies which are far simpler and less time-consuming than those of other mesostructured materials of the M41S family.

References

[1] J.M. Thomas, Angew. Chem. Int. Ed. Engl. 33 (1994) 913.
[2] J.S. Beck, J.C. Vartuli, W.J. Roth, M.E. Leonoswicz, C.T. Kresge, K.D. Schmitt, C.T.-W. Chu, D.H. Olson, E.W. Sheppard, S.B. McCullen, J.B. Higgins, J.L. Schlenker, J. Am. Chem. Soc. 114 (1992) 10834.
[3] C.T. Kresge, M.E. Leonowicz, W.J. Roth, J.C. Vartuli, J.S. Beck, Nature 359 (1992) 710.
[4] S. Inagaki, Y. Fukushima, K. Kuroda, J. Chem. Soc., Chem. Commun. (1993) 680.
[5] A. Tuel, S. Gontier, Chem. Mater. 8 (1996) 114.
[6] Q. Huo, D.I. Margolese, G.D. Stucky, Chem. Mater. 8 (1996) 1147.
[7] S.A. Bagshaw, E. Prouzet, T.J. Pinnavaia, Science 269 (1995) 1242.
[8] R. Ryoo, J.M. Kim, C.H. Shin, J.Y. Lee, Stud. Surf. Sci. Catal. 105 (1997) 45.
[9] P. Behrens, Angew. Chem. Int. Ed. Engl. 35 (1996) 515.
[10] C. Rizzo, A. Carati, M. Tagliabue, C. Perego, Stud. Surf. Sci. Catal. 128 (2000) 613.
[11] G. Bellussi, C. Perego, A. Carati, S. Peratello, E. Previde Massara, G. Perego, Stud. Surf. Sci. Catal. 84 (1994) 85.
[12] J.M. Thomas, W.J. Thomas, Principles and Practice of Heterogeneous Catalysis, VCH, Weinheim, 1997.
[13] G. Perego, R. Millini, G. Bellussi, in: H.G. Karge, J. Weitkamp (Eds.), Molecular Sieves, vol. 1, Springer, Berlin, 1998, p. 187.
[14] M. Boudart, Top. Catal. 13 (2000) 147.
[15] C. Louis, M. Che, in: G. Ertl, H. Knözinger, J. Weitkamp (Eds.), Handbook of Heterogeneous Catalysis, vol. 1, VCH, Weinheim, 1997, p. 207.
[16] I.M. Campbell, Catalysis at Surfaces, Chapman & Hall, London, 1988, p. 4.
[17] W.F. Hoelderich, Catal. Today 62 (2000) 115.
[18] C. Berlini, G. Ferraris, M. Guidotti, G. Moretti, R. Psaro, N. Ravasio, Micropor. Mesopor. Mater. 44–45 (2001) 595.
[19] A. Corma, M.T. Navarro, J. Pèrez-Pariente, J. Chem. Soc., Chem Commun. (1994) 147.
[20] T. Blasco, A. Corma, M.T. Navarro, J. Pérez Pariente, J. Catal. 156 (1995) 65.
[21] F. Di Renzo, H. Cambon, R. Dutartre, Micropor. Mater. 10 (1997) 283.
[22] C. Berlini, M. Guidotti, G. Moretti, R. Psaro, N. Ravasio, Catal. Today 60 (2000) 219.
[23] T. Maschmeyer, F. Rey, G. Sankar, J.M. Thomas, Nature 378 (1995) 159.
[24] R.D. Oldroyd, G. Sankar, J.M. Thomas, D. Özkaya, J. Phys. Chem. B 102 (1998) 1849.
[25] G. Moretti, C. Dossi, A. Fusi, S. Recchia, R. Psaro, Appl. Catal. B 20 (1999) 67.
[26] J. Livage, Stud. Surf. Sci. Catal. 85 (1994) 1.
[27] A. Carati, C. Rizzo, M. Tagliabue, C. Perego, Stud. Surf. Sci. Catal. B 130 (2000) 1085.
[28] P.J. Branton, P.G. Hall, K.S.W. Sing, J. Chem. Soc., Chem. Commun. (1993) 1257.
[29] J.D. Carruthers, P.A. Cutting, R.E. Day, M.R. Harris, S.A. Mitchell, K.S.W. Sing, Chem. Ind. 50 (1968) 1772.
[30] L. Marchese, T. Maschmeyer, E. Gianotti, S. Coluccia, J.M. Thomas, J. Phys. Chem. B 101 (1997) 8836.
[31] C. Perego, S. Amarilli, A. Carati, C. Flego, G. Pazzuconi, C. Rizzo, G. Bellussi, Micropor. Mesopor. Mater. 27 (1999) 345.
[32] G. Bellussi, C. Perego, S. Peratello, US Patent 5,342,814 (1994).
[33] S. Peratello, M. Molinari, G. Bellussi, C. Perego, Catal. Today 52 (1999) 271.
[34] A. Carati, C. Perego, L. Dalloro, G. De Alberti, S. Palmery, IT 1996—MI1499.
[35] V. Calemma, S. Peratello, C. Perego, A. Moggi, R. Giardino, Proceedings of the 218th National Meeting ACS, vol. 44, no. 3, 1999, p. 241.
[36] M. Guidotti, G. Moretti, R. Psaro, N. Ravasio, Chem. Commun. (2000) 1789.